SAND95-1731C
CONF-951155--25

REAL TIME MEASUREMENT OF EPILAYER STRAIN USING A SIMPLIFIED WAFER CURVATURE TECHNIQUE

J. A. FLORO, E. CHASON, and S. R. LEE
Sandia National Laboratories, Albuquerque, NM, 87185-1415, jafloro@sandia.gov

ABSTRACT

We describe a technique for measuring thin film stress using wafer curvature that is robust, compact, easy to setup, and sufficiently sensitive to serve as a routine diagnostic of semiconductor epilayer strain in real time during MBE or CVD growth. We demonstrate, using growth of SiGe alloys on Si, that the critical thickness for misfit dislocation can clearly be resolved, and that the subsequent strain relaxation kinetics during growth or post-growth annealing are readily obtained.

INTRODUCTION

The bandstructure and transport properties of electronic and optoelectronic materials can be significantly modified by the presence of coherency strain associated with the pseudomorphic heteroepitaxial growth of the material on a substrate with a different lattice parameter. Device designers take advantage of this effect in the fabrication of novel high performance devices using strained alloy or compound semiconductor thin films typically grown by molecular beam epitaxy (MBE) or by chemical vapor deposition (CVD). Monitoring and controlling the degree of strain (which is determined by the epilayer composition, the substrate lattice parameter, and the degree of strain relaxation) is a significant challenge to the epilayer grower. An in situ diagnostic that can determine the strain state in real time during growth or subsequent thermal annealing would clearly be of great utility, especially if the diagnostic can operate in the CVD environment as well as in the MBE environment.

In this paper we describe a technique for epilayer strain determination. We measure the curvature of the underlying substrate to determine the stress, and therefore the strain, of the epilayer in real time during growth. The technique uses a laser as a probe, and is thus compatible with both the CVD and MBE environments (as long as optical access to the substrate is available). While curvature-based stress measurements have found wide application in the broader thin films community, relatively little use of this approach has been made within the semiconductor epilayer growth community. We have designed our particular variation of the curvature technique with robustness, compactness, and ease of use for the grower as our primary goals. We first briefly discuss the relevant background and prior art in this area, and then describe our approach. After examining the strain sensitivity of this technique, we present an example of its capabilities using SiGe MBE growth as a demonstration.

An alternative technique applicable to MBE growth is Reflection High Energy Electron Diffraction (RHEED). RHEED measures the surface lattice parameter of a growing epilayer, which is often the quantity of greatest interest, especially when a compositionally graded, partially relaxed buffer layer is being grown. Several measurements of the surface lattice parameter during III-V epilayer growth have been presented [1,2]. The advantages of the laser curvature technique are: (1) useful in the typical high pressure CVD environment; (2) insensitivity to stray electric and magnetic fields, making the technique easier to use when high-current sample heaters are in use, or when electron-beam evaporators are employed as deposition sources (e.g., for Si deposition); and (3) routine use is simple with no knowledge of diffraction required.

MASTER
DISTRIBUTION OF THIS DOCUMENT IS UNLIMITED

BACKGROUND AND PRIOR ART

A biaxially strained thin film rigidly attached to a much thicker substrate induces a curvature $\kappa = 1/R$, where R is the radius of curvature, given by [3,4]

$$\kappa - \kappa_0 = \frac{M_f h_f \varepsilon}{6 M_s h_s^2}, \quad (1)$$

where ε is the biaxial strain, $M_{f,s}$ are the film, substrate biaxial moduli, and $h_{f,s}$ are the film, substrate thicknesses. κ_0 is the initial curvature of the substrate prior to film growth. Curvature resolution is clearly enhanced by reducing substrate thickness. Note that it is the film stress $\sigma = M_f\varepsilon$ that is determined directly from a curvature measurement. Determining film strain requires knowledge of the biaxial modulus of the film.

There are many ways in which to measure the curvature of a substrate. We focus here on the deflection of a laser beam incident on multiple points on the sample. The deflection arises from the spatially varying surface normal of the film/substrate combination due to its stress-imposed curvature. As discussed below, we monitor the deflection of multiple parallel laser beams using a CCD array detector. This is in contrast to the laser scanning techniques, where a single laser beam is moved point-to-point across a sample, typically through use of a rotating mirror [5]. The laser is located exactly at the focal plane of a long focal length lens, thus converting the angular scan of the mirror into a linear scan across the sample. A position sensitive detector (PSD) is also located at the focal plane of the same lens. In this configuration, the scanned beam will arrive at the same point on the PSD if the wafer is flat. A uniformly curved wafer produces a constant deflection during scanning that is proportional to the curvature. This technique is sensitive and is sufficiently rapid to perform real-time measurements. It has been applied, for example, to the measurement of strain relaxation kinetics of SiGe alloys on Si during growth [6] and furnace annealing [7]. The primary drawbacks to this technique are associated with matters of operational convenience, in particular the need for precise alignment of the laser and PSD relative to the lens, and the use of a rotating mirror. An alternative approach to laser scanning is to use two stationary laser beams (e.g., produced by a single laser and a beamsplitter) and measure their separation using quadrant photodiodes [8]. The change in beam spacing with time is again directly proportional to the wafer curvature. The technique is simple, sensitive, and robust. The only drawback is that only two points are sampled. In the next section we describe two modifications to this approach that further refine the ease of use and setup.

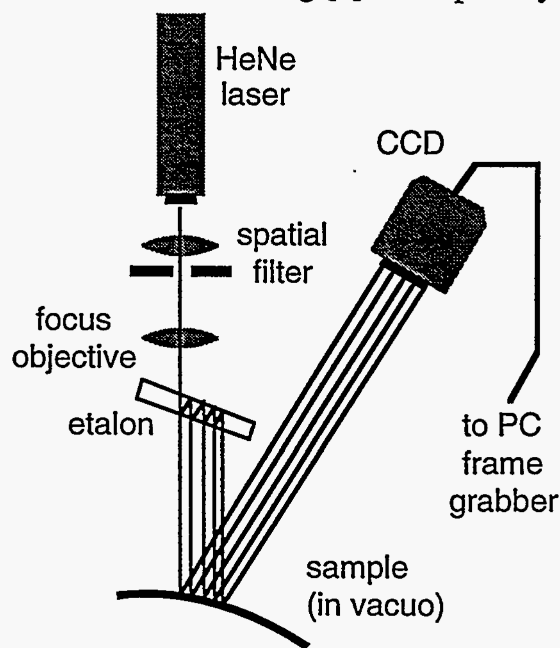

Figure 1. Schematic setup of the curvature measurement technique.

THE TECHNIQUE

Our generic setup is shown in Fig. 1. A single polarized HeNe laser beam is converted into multiple parallel beams through use of a highly reflective etalon. The output beam spacing is determined by the angle between the laser beam axis and the surface normal of the etalon. We typically employ five - a practical limit on the number of beams arises from the reduced intensity of each subsequent beam. For an etalon with surfaces of reflectivity R, $I_n/I_1 = R^{2(n-1)}$, where I_n is the

intensity of the nth transmitted beam and I_1 is the intensity of the first transmitted beam. In the experiments presented here, $R = 0.9$ and hence $I_5/I_1 = 0.43$. Higher reflectivity etalons reduce the relative intensity loss I_5/I_1 at the expense of also reducing the absolute intensity.

After reflection from the sample, the beams are detected on a Peltier-cooled CCD camera. The only other optics employed are a spatial filter (lens and pinhole) to "clean up" the beam profile, and a focusing objective that focuses the beam on the camera. Additional attenuators may be necessary to reduce the beam intensity to avoid saturating the CCD. The use of a CCD permits simple detection of more than two beams. In addition, the CCD camera allows for easy focusing of the beams, which is important for obtaining maximum sensitivity. Finally, commercial acquisition hardware and software are readily available [9]. The primary drawbacks are the "digitization" of the analog beam distribution, which reduces spatial resolution, and the limited size of the CCD array, which limits the maximum sample region to be probed.

In order to determine the substrate curvature we measure the spacing between each adjacent beams D. Curvature is determined from the differential spacing $\Delta D/D_0$ by

$$\frac{\Delta D}{D_0} = \frac{2L\kappa}{\cos\alpha}, \qquad (2)$$

where $D_0 = D(t{=}0)$, $\Delta D = D(t) - D_0$, L is the length from sample to CCD array, and α is the angle of incidence on the sample ($\alpha = 0°$ for normal incidence). Spatially resolved curvature measurements are obtained by tracking each differential spacing independently. For the purposes of this paper we spatially average over all the measured spacings to arrive at one mean differential spacing $\langle\Delta D/D_0\rangle$ and thus one average curvature.

The laser beam positions on the CCD array are determined through use of PC-based image acquisition software and hardware originally developed for RHEED applications [9]. A "window" is placed around each laser spot on the CCD image. Periodically the frame grabber acquires the full image and determines the centroid of the intensity distribution within each window. The row and column position of the centroid is then written to disk. The software allows each window to track the centroid, preventing loss of accuracy due to curvature- or drift-induced beam motion. Currently the software permits real-time data acquisition, but does not analyze or display quantities such as the differential spacing or the strain in real time. Thus, after growth the time-varying centroid positions are differenced to get the spacings D(t).

One requirement in order to accurately determine the strain from measurements of the substrate curvature is that the sample be mounted such that the bending of the substrate is unconstrained. We have used a "cage" about the perimeter of the sample that allows the sample full bending freedom, allows for RHEED access, and permits backside radiative heating.

SENSITIVITY

In order to determine the sensitivity and resolution of the setup, we measure the mean differential spacing on a static (no growth) 2" diameter Si wafer, 0.28 mm thick, as a function of time. In this case the mean differential spacing fluctuates about zero. The maximum resolvable radius of curvature R_{max} is then determined by taking $\langle\Delta D/D_0\rangle$ to be twice the standard deviation of the fluctuations in the signal. The laser apparatus is mounted on a turbopumped MBE (with no special provisions for vibration reduction or isolation) with a relatively compact sample-to-CCD distance of L = 66 cm and $\alpha = 3°$. We find $\langle\Delta D/D_0\rangle_{static} = 0.0004$, which, from equation 2, gives $R_{max} = 1.7$ km. Using equation (1) we can relate R_{max} to the minimum resolvable thickness of an epilayer with a strain ε. For demonstration purposes we will calculate this using values appropriate to the SiGe/Si experiments to be described in the next section. Taking $h_s = 0.28$mm, $M_{Si} = 180.4$ GPa, and $M_{Ge} = 168.9$ GPa (and interpolating the alloy modulus using the rule of mixtures), h_f^{min} vs. ε is calculated and plotted in Fig. 2. As an example of the interpretation of this curve, we see

that for a film with 1% strain ($Si_{75}Ge_{25}$), 6 monolayers of film are detectable, and for a film with 4% strain, 2 monolayers are detectable. Conversely, for a film 200 Å thick, strains less than 0.1% can be resolved. For comparison, we also plot in Fig. 2 the equilibrium critical thickness [10] for misfit dislocation formation. We find that the critical thickness curve lies everywhere above the h_f^{min} curve, implying that for any $Si_{(1-x)}Ge_x$ composition we have sufficient resolution to detect the equilibrium critical thickness. Clearly, however, the sensitivity depends strongly on the substrate thickness. We may generalize beyond SiGe by considering both the specific form of the epitaxial critical thickness h_c (we use here the form given by Freund [11]) and the minimum resolvable epilayer thickness h_{min} from the curvature measurement:

$$h_c = \frac{b\left(1-\cos^2\beta\right)\ln\left(2h_c/r_0\right)}{8\pi(1+\nu)\sin\alpha\sin\beta\,\varepsilon}, \qquad h_{min} = \frac{M_s h_s^2}{6 M_f R_{max}\varepsilon}, \qquad \text{(3a), (3b)}$$

where b is the Burgers vector, ν is Poisson's ratio, $\alpha = 54.74°$ and $\beta = 60°$ for (001) epitaxy, r_0 is the dislocation core cutoff width, and all other quantities are as defined previously. In order to detect the critical thickness by our technique, we must have $h_c/h_{min} \geq 1$. If we take the ratio of equations 3a and 3b, and substitute $\nu = 1/3$, the values of α and β given above, and we approximate $h_c = 10r_0$ in the logarithmic term (since we are concerned with small critical thicknesses), we arrive at

$$\frac{bR_{max}}{h_s^2}\left(\frac{M_f}{M_s}\right) \geq 1.44 \qquad (4)$$

If we further take $M_f = M_s$, $R_{max} = 1.7$ km, and b = 2 Å, and solve for the substrate thickness, we get $h_s < 0.49$ mm in order to resolve the critical thickness for a typical heteroepitaxial semiconductor system. If thicker substrates are used, then the sensitivity must be increased. This may be attained by increasing the sample-to-CCD distance L (equation (2)), although the actual gain in sensitivity depends on the source of the noise.

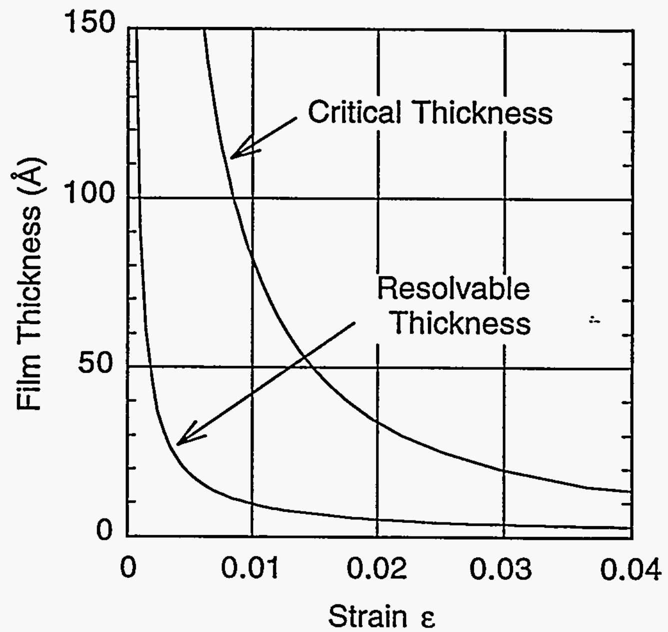

Figure 2. Thickness/strain sensitivity curve for SiGe on 0.28 mm Si (001) substrates. Also plotted is the equilibrium critical thickness curve for SiGe/Si.

HETEROEPITAXIAL GROWTH OF SiGe

During growth, the differential spacing is related to the strain and film thickness by

$$\frac{\Delta D}{D_0} = F\varepsilon(t)h_f, \qquad F = \frac{12LM_f}{M_s h_s^2 \cos\alpha}, \qquad \text{(5a), (5b)}$$

where we recognize that the strain can be time dependent during the relaxation regime. Prior to relaxation the strain is constant and the differential spacing will vary linearly with thickness. Thus, unlike RHEED, we obtain a positive determination that a coherently strained layer is growing.

In order to demonstrate the real time capabilities of the technique, we grow uniform SiGe alloys of composition 29% Ge (1.2% strain), and total deposition rate 0.6 Å/s. Composition is verified by x-ray diffraction measurements and the final thicknesses by RBS. The substrates consist of sections of 2" diameter Si (001) wafers, 0.28 mm thick. The substrates are chemically cleaned, leaving a final weakly-bound oxide passivated surface. The oxide is desorbed in situ at 830°C and a 1200Å Si buffer is grown at 700°C. Surface quality and reconstruction is monitored by RHEED. A smooth, 2x1 reconstructed surface serves as the starting point for alloy growth. The substrate is equilibrated at the growth temperature (measured by pyrometer) for at least one hour. Deposition is accomplished with electron beam evaporators. Prior to opening the shutters to expose the substrate to the growth fluxes, the laser spot positions are measured for 100 seconds to determine the initial spacings D_0. The laser enters and exits through a standard glass viewport.

In Fig. 3 we show the mean differential spacing as a function of film thickness for alloys grown at three temperatures. These measurements were carried out to much larger thicknesses, but we concentrate on the early stages of growth to highlight the deviation from linearity. For all three layers the mean differential spacing initially varies linearly with thickness, indicating fully coherent growth. All three curves eventually become sublinear, with the deviation occurring at greater thicknesses for lower growth temperatures. The points at which deviation occurs define the kinetically limited critical thicknesses. For the film grown at 650°C, the critical thickness appears to be very close to the equilibrium value predicted by equation (3a). Thus we are easily able to map out the critical thickness as a function of growth temperature, and to verify the equilibrium h_c

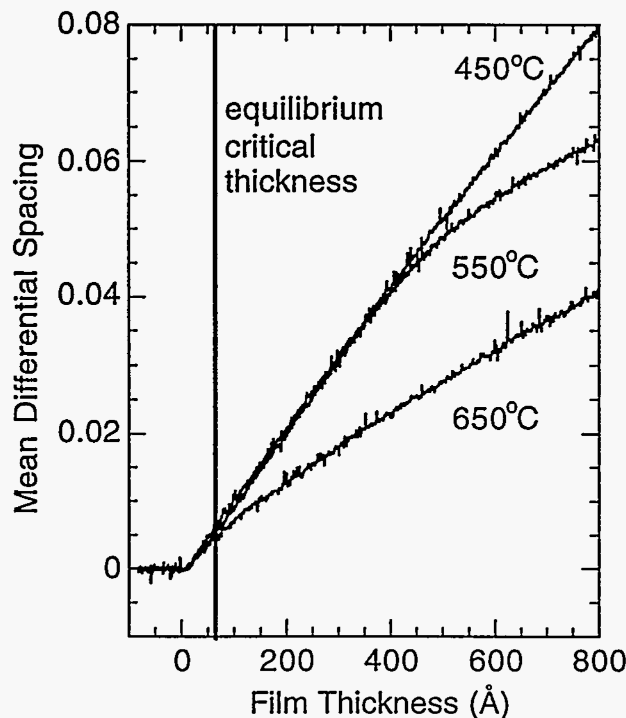

Figure 3. Mean differential spacing vs. film thickness for $Si_{71}Ge_{29}$ epilayers during growth on Si (001), for three growth temperatures.

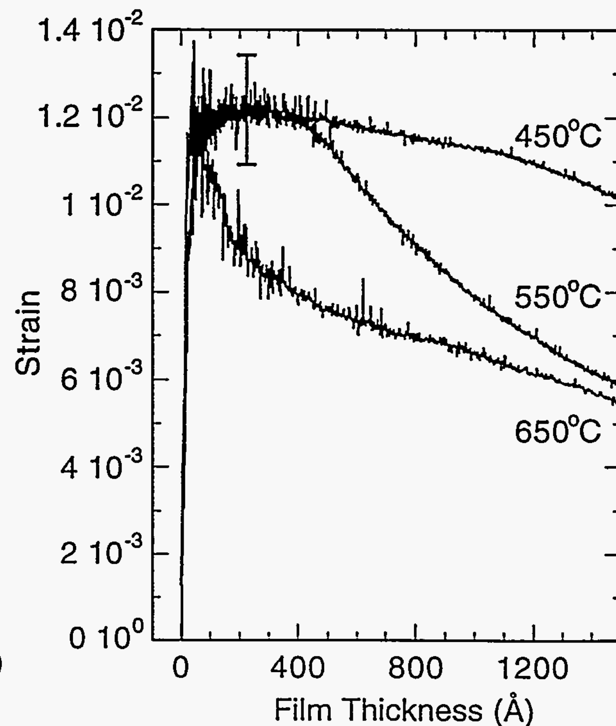

Figure 4. Strain in $Si_{71}Ge_{29}$ epilayers during growth on Si (001), for three growth temperatures.

by growing at sufficiently high temperature.

In Fig. 4 we plot strain vs. film thickness for the same three films shown in Fig. 3. The strain is obtained by inverting equation (5a). The plateau regions at low thicknesses correspond to the coherent regime. Past the critical thickness, an S-shaped relaxation profile representing the nucleation and glide of misfit dislocations is observed. The final degree of relaxation in the films has also been verified ex situ by x-ray diffraction. We note that the accuracy in the absolute determination of the strain is limited by the accuracy to which the parameter F in equation (5) is known. This is typically dominated by error in substrate thickness measurement. The error bar in Fig. 4 represents a $\pm$ 5 μm error in substrate thickness.

Finally we note that the mean differential spacing is the most sensitive parameter for determining the critical thickness, while the strain vs. thickness (or time) is best suited for evaluation relaxation kinetics.

CONCLUSIONS

We have developed a technique for measuring substrate curvature, and thus film strain, that is robust, compact, easy to set up, and sufficiently sensitive to routinely evaluate epilayer critical thicknesses and strain relaxation kinetics. The technique can be used in both MBE and CVD growth environments, as long as optical access is available and the substrate is free to bend. The technique has been designed as an in situ, real time diagnostic of semiconductor heteroepitaxy, but can also be used to determine strain during growth of polycrystalline and amorphous materials (unlike RHEED). The curvature technique only determines an average strain over the thickness of the epilayer, which may be a limitation for graded layers or multilayers. Nonetheless, the simplicity and sensitivity of this approach should make it a useful diagnostic in a variety of growth situations.

ACKNOWLEDGMENTS

Our thanks to Mike Sinclair and Carl Seager for optics advice, and to Jay Penn for assistance with the setup and MBE growth. We are grateful to Darryl Barlett of k-Space Associates for timely modifications to his software. This work was performed at Sandia National Labs and supported by the U. S. Department of Energy under contract DE-AC04-94AL85000.

REFERENCES

1. J. Mirecki-Millunchick and S. A. Barnett, Appl. Phys. Lett. **65** 1136 (1994)
2. G. J. Whaley and P. I. Cohen, Appl. Phys. Lett. **57**, 144 (1990).
3. G. G. Stoney, Proc. R. Soc. London Ser. A **82**, 172 (1909).
4. P. H. Townsend, D. M. Barnett, and T. A. Brunner, J. Appl. Phys. **62**, 4438 (1987).
5. Paul A. Flinn, Donald S. Gardner, and William D. Nix, IEEE Trans. Electron Devices **ED-34**, 689 (1987).
6. Veronique T. Gillard and William D. Nix, Zeitschrift fur Metallkunde **84**, 874 (1993).
7. C. A. Volkert, E. A. Fitzgerald, R. Hull, Y. X. Hie, and Y. J. Mi, J. Elec. Mater. **20**, 833 (1991).
8. A. J. Schell-Sorokin and R. M. Tromp, Phys. Rev. Lett. **64**, 1039 (1990).
9. k-Space Associates, Inc., 2231 Stone Drive, Ann Arbor, MI 48105.
10. L. B. Freund, J. Mech. Phys. Solids **38**, 657 (1990).